THERMAL ANOMALY IN MARTIAN NORTH POLAR ERG LIKELY DUE TO NEAR-SURFACE ICE.

N. E. Putzig[1], M. T. Mellon[2], K. E. Herkenhoff[3], R. J. Phillips[1], B. J. Davis[1], and K. J. Ewer[4]. [1]Southwest Research Institute, Planetary Science Directorate, Boulder, CO (contact: nathaniel@putzig.com); [2]University of Colorado, Laboratory for Atmospheric and Space Physics, Boulder, CO; [3]United States Geological Survey, Astrogeology Team, Flagstaff, AZ; [4]Embry-Riddle Aeronautical University, Prescott, AZ.

Synopsis: A wider range of thermal observations and forward modeling of heterogeneity are used to show that a long-standing thermal discrepancy in the north polar erg is consistent with normal basaltic sand overlying shallow ground ice, obviating the need to invoke sand-sized agglomerations of dust.

Background: The north polar layered deposits are surrounded by dark dunes known as the circum-polar erg (Fig. 1a) and are likely related to climate variations [1,2]. Neutron data suggest that water ice is present within a meter of the erg's surface [3], additionally constraining climate. Dunes of similar morphology, color, and albedo at lower latitudes [4] have thermal inertia (~250 tiu [J m^{-2} K^{-1} $s^{-1/2}$]) consistent with sand-sized basaltic grains [5,6,7]. In the erg, much lower values (~75 tiu) suggestive of dust-sized grains were reported [8,9]. A widely accepted solution to this discrepancy is bonding of fines into larger, low-density aggregate particles capable of forming dunes [10,11], perhaps as they are weathered out of the layered deposits [1,2,11] or the underlying units [12,13].

Thermal inertia and heterogeneity: Modeling studies show that surface heterogeneity may cause anomalous thermal behavior [14,15], allowing an alternative explanation for the thermal properties of the erg. Counterintuitively, certain configurations of near-surface layering may produce apparent thermal inertia (derived assuming constant properties) that is substantially lower than the intrinsic thermal inertia of both the surface layer and its substrate [15]. Thus, the polar erg may be surfaced by ordinary basaltic sand (with up to 30 wt% gypsum [16]), its low apparent thermal inertia attributable to an effect of surface heterogeneity due to the icy substrate.

Diurnal and seasonal variations in apparent thermal inertia indicate that heterogeneity is widespread globally, consistent in the polar region with layering (Fig. 1b,c) [17]. The use of both nighttime and daytime observations is a key element of this analysis, especially near the poles where seasons free of CO_2 ice largely correspond to those when the Sun is predominantly above the horizon.

Heterogeneity at Phoenix and in the polar erg: At the Phoenix landing site, seasonal and diurnal variations in apparent thermal inertia as derived from Mars Global Surveyor Thermal Emission Spectrometer (TES) data can be modelled well by ~4 cm of sand overlying ground ice (Fig. 2a), consistent with the observations made from the lander [18]. When the model sand thickness approaches or exceeds a diurnal skin depth (1/26 of the seasonal skin depth), the 2AM apparent thermal inertia can be substantially less than that of the sand. Thus, the thermal inertia of surface materials may be underestimated if one uses nighttime only or annual-mean values fit to diurnal temperatures, as was done with Viking data.

At the higher latitudes of the polar erg, seasons of useful TES data are more restricted than at Phoenix, and their variations are larger (Figs. 2b-d). To resolve

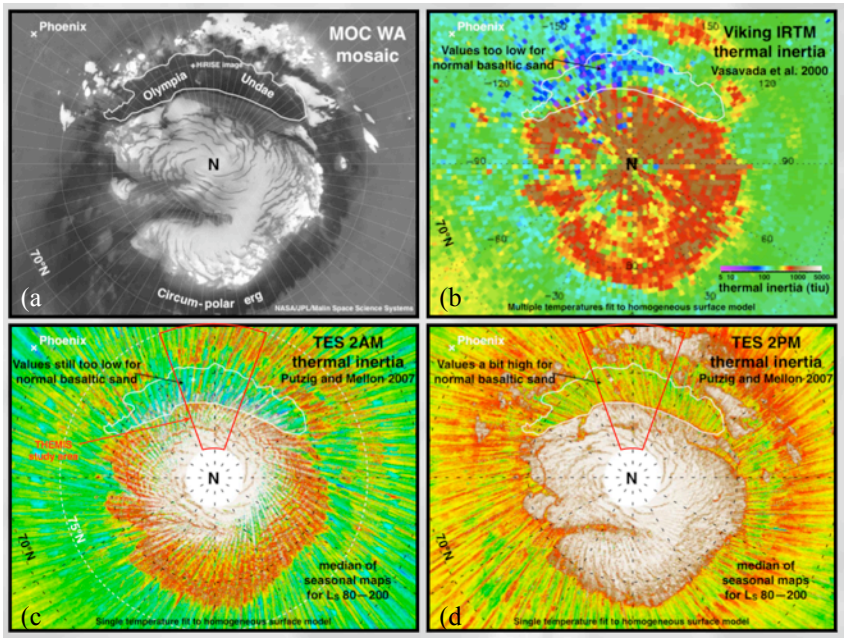

Figure 1. North polar region, 65–90°N, 0°W at bottom. (a) Mosaic of MOC wide-angle images; polar erg is irregular, dark material surrounding bright polar layered deposits. (b) Thermal inertia derived from Viking data [9]. Low values, especially in Olympia Undae, were seen as more consistent with dust than with sand. (c) 2AM and (d) 2PM annual-median apparent thermal inertia derived from TES data [17]. Streaks aligned with orbit tracks are due to seasonal variations. Thermal inertia scale same as in (b).

these short-term, rapid changes, we remapped the north polar region with a finer seasonal increment of 5° L_S (cf. 10° used in Fig. 2a and globally by [17]). This change allows better discrimination between models for matching to the observed thermal behavior. We found the TES results for the erg to be most consistent with a sand layer of ~15-25 cm (Fig. 2b), with dust-layer models yielding poorer fits (Fig 2c). Between dune crests in the erg, HiRISE images show brighter, possibly consolidated materials that may have higher thermal inertia. However, the best-fitting models of this type (70:30 mixture of dust and rock; Fig. 2d) do not capture the observed thermal behavior.

THEMIS thermal inertia: We investigated the derivation of thermal inertia from Thermal Imaging Spectrometer (THEMIS) Band 9 images for the north polar region. At 100 m/pixel (cf. TES at ~3 km/pixel), THEMIS data may allow better discrimination between heterogeneity models. We derived thermal inertia from a selection of THEMIS images of Olympia Undae to produce the maps in Fig. 3. The nighttime results show a pattern of high and low values in the erg and its surroundings that is grossly similar to that of TES 2AM maps, but with lower median values. In contrast, the daytime results show dramatically higher values of thermal inertia. However, these images may have been affected by partial CO_2-frost cover on the ground at these earlier seasons. The lack of coverage for later seasons hampers the incorporation of daytime results into our analysis at this time. Since THEMIS continues to acquire images (now at times of day more favorable for thermal analysis), we hope to eventually obtain broader seasonal coverage.

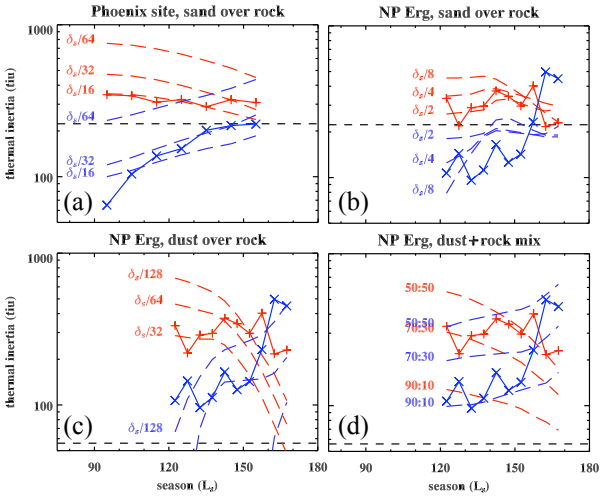

Figure 2. 2AM (blue) and 2PM (red) apparent thermal inertia from TES (×, + symbols) and from various models (dashed curves) of sand or dust and rock (i.e., ground ice) at (a) the Phoenix site (× in Fig. 1) and (b-d) in the polar erg (+ in Fig. 1) during summer seasons. Horizontal dashed lines represent sand (223 tiu) or dust (56 tiu). Labels in (a-c) are upper-layer thickness in fractional seasonal skin depth, δ_S (70 cm for sand, 21 cm for dust). Labels in (d) are dust:rock mixing ratio. Models in (a) and (b) provide the best fits, with ~4 cm and ~20 cm of sand at Phoenix and at the erg site, respectively. Next-best models of dust-rock (c) layering and (d) mixing have larger deviations from the TES results.

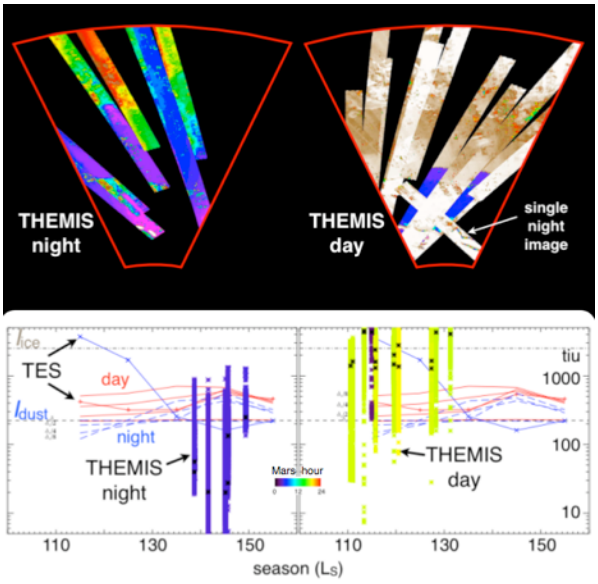

Figure 3. Thermal inertia from THEMIS Band 9 for 160°-200°E, 75°-87°N. Thermal-inertia color scale same as for Fig. 1. Graphs are for Olympia Undae (center of maps, 79-83N) with values extracted from THEMIS images (* symbols, where colors are local time of day and black is median value within each image), median values from TES (x, + symbols), and results from layered models of sand over ice-cemented soil (solid and dashed colored lines). Large THEMIS image-to-image variations and extreme values relative to TES are not fully explained but may be related to suboptimal observing conditions and larger instrument error, particularly for daytime images.

References: [1] Thomas P. et al. (1992) in: *Mars*, Kieffer H.H. et al. (1992) U. AZ Press. [2] Clifford S.M. et al. (2000) *Icarus 144*, 210–242. [3] Feldman W.C. et al. (2008) *Icarus* 196, 422-432. [4] Thomas P. & Weitz C. (1989) *Icarus 81*, 185-215. [5] Sagan C. & Bagnold R.A. (1975) *Icarus 26*, 209-218. [6] El-Baz F. et al. (1979) *JGR 84*, 8205-8221. [7] Breed C.S. et al. (1979) *JGR 84*, 8183-8204. [8] Paige D.A. et al. (1994) *JGR 99*, 25,959–25,991. [9] Vasavada A.R. et al. (2000) *JGR 105*, 6961–6969. [10] Herkenhoff K.E. & Vasavada A.R. (1999) *JGR 104*, 16,487–16,500. [11] Cutts J.A. et al. (1976) *Science 194*, 1329-1337. [12] Byrne S. & Murray B.C. (2002) *JGR 107*, E6, 5044. [13] Fishbaugh K.E. & Head J.W. (2005) *Icarus 174*, 444-474. [14] Putzig N.E. & Mellon M.T. (2007) *Icarus 191*, 52-67. [15] Mellon M.T. & Putzig N.E. (2007) *LPS XXXVIII*, Abstract #2184. [16] Horgan et al. (2009) *JGR* 114, E01005. [17] Putzig N.E. & Mellon M.T. (2007) *Icarus 191*, 68-94. [18] Mellon M.T. et al. (2009), *JGR 114*, E00E07.